Journal of Science and Sustainable Development (JSSD), 2026, 14(2), 39-59

ISSN: 2304-2702 (print); 2414-4479 (online)
DOI: 10.20372/au.jssd.14.2.2026.0752

RESEARCH PAPER

Integrated Assessment of Land Use/Land Cover Dynamics and Climate Change Impacts on Watershed Hydrology in the Dawe Watershed, Ethiopia

Birhanu Legesse Wakjira[1]*, Asfaw Kebede Kassa[2], Awdenegest Moges[3], Olkeba Tolessa Leta[4]

[1]*Ph.D. candidate, Department of Natural Resources Management, Ambo University, Ethiopia. birelegesse2000@gmail.com, https://orcid.org/0009-0008-7237-4315*
[2]*Haramaya Institute of Technology, Ethiopia. asfaw649@gmail.com, https://orcid.org/0000-0002-6496-7216*
[3]*Department of Agricultural Engineering, Hawassa University, Ethiopia. awde_moges@yahoo.co.uk, https://orcid.org/0000-0001-6084-8327*
[4]*St. Johns River Water Management District, Palatka, FL, United States. olkebat2005@gmail.com, https://orcid.org/0000-0003-3479-901X*

***Corresponding author**: birelegesse2000@gmail.com

Abstract

Freshwater sustainability is increasingly threatened by the impacts of land use/land cover (LULC) dynamics and climate changes, mainly in arid and semi-arid data-scarce watersheds of developing countries. This study assessed the separate and combined effects of predicted LULC dynamics and climate changes on the water resources in the Dawe watershed, Ethiopia. Future LULC was projected using a Cellular Automata (CA)-Markov model, while climate projections were derived from an ensemble of six CMIP6 Global Climate Models (GCMs) under the shared socioeconomic pathways (SSPs) SSP2–4.5 and SSP5–8.5. Hydrological responses were simulated using the Soil and Water Assessment Tool Plus (SWAT+) under nine scenarios (S0–S8), integrating projected LULC conditions (2024 and 2062) with mid-century (2024–2055) and late-century (2056–2085) climate projections. With Nash-Sutcliffe efficiency (NSE) and Kling-Gupta efficiency (KGE) values surpassing 0.8 during both calibration and validation, the model demonstrated strong performance. The simulations demonstrate a consistent increase in evapotranspiration (ET) under all scenarios, ranging from 13.0% under climate change alone (S1) to 23.4% under the combined LULC and climate change scenario (S8). In contrast, water yield (WY), surface runoff (SR), and groundwater recharge (GWR) will decline under all future scenarios, with the greatest reduction occurring under the combined effects of LULC and climate change. Under the worst-case scenario (S8: SSP5–8.5, 2062 LULC, and late-century climate), WY decreased by 34.5%, SR by 32.9%, and GWR by 23.2%. The continued land expansion and warming will alter watershed hydrology. Climate change is the main driver of hydrological shifts, amplified by LULC change. The worst impacts occur under combined SSP5–8.5 and 2062 LULC, so assessing drivers separately underestimates risks, underscoring the need for integrated modeling. These results highlight the necessity of integrated land and water resource management strategies to enhance water security and strengthen climate resilience.

Keywords: CMIP6, SWAT+, SSP, LULC dynamics, climate change, Dawe watershed.

Introduction

Freshwater resource is fundamental to sustain life on the globe. However, it is increasingly threatened by the effect of land use/land cover (LULC) dynamics and climate change. According to the Intergovernmental Panel on Climate Change (IPCC), rising temperatures, altered precipitation regimes, increasing climate variability, rapid population growth, and accelerating land degradation are intensifying water scarcity worldwide, with the greatest impacts occurring in semi-arid and arid regions (IPCC, 2023).

The impacts of these environmental changes are particularly pronounced in Sub-Saharan Africa, where livelihoods and national economies depend heavily on climate-sensitive sectors such as rain-fed agriculture (Shah et al., 2008). Moreover, limited adaptive capacity, rapid population growth, and increasing pressure on natural resources further heighten the vulnerability of the region to hydrological extremes (IPCC, 2023). Ethiopia is the most climate change affected nation in the region, mainly because of its dependence on rain-fed agriculture (Feleke *et al*., 2025; Gebrechorkos *et al*., 2019). In recent decades, the country has experienced recurrent droughts, increasing erratic rainfall, rising temperatures, and continuous degradation of natural vegetation, resulting in declining water availability, reduced agricultural productivity and increasing food insecurity (Amsalu, 2019; Aragaw *et al*., 2021).

Beyond climate change, LULC dynamics have emerged as major drivers of hydrological change. Human-induced land transformations, including agricultural expansion, deforestation, urbanization, and overgrazing, substantially modify watershed hydrological processes by altering interception, infiltration, evapotranspiration, runoff generation, and groundwater recharge (Birhanu *et al*., 2022; Kuma *et al*., 2022). In Ethiopia, the rapid conversion of forests, shrublands, and wetlands into cultivated and built-up areas has accelerated over the last few decades (Ayalew and Nigussie, 2023; Wudineh, 2023). The prevailing water resources scarcity is being exacerbated by the intensified soil erosion, reduced ecosystem resilience, and diminished capacity of watersheds to regulate stream flow and recharge groundwater.

Climate change and LULC change are closely interrelated and often reinforce each other. Climate change influences LULC through changes in vegetation distribution, agricultural practices, drought frequency, and land degradation. However, LULC changes contribute to climate change by altering surface energy balance, reducing carbon sequestration, and increasing greenhouse gas emissions through deforestation and urban expansion (Bikeko and Venkatesham, 2024; FAO, 2023; Yang *et al*., 2024). Their combined impacts produce nonlinear hydrological responses that differ substantially from the impacts of either driver alone. As a result, assessing these factors separately could underestimate future shifts in watershed hydrology and water availability.

The Dawe watershed, located in the northeastern Wabi-Shebelle River Basin (WSRB) in eastern Ethiopia, is experiencing the impact of LULC dynamics and climate changes (Harka *et al*., 2020). The watershed is facing water scarcity because of the combined influence of climate variability, rapid urbanization, agricultural expansion, and environmental degradation (Engdaw, 2016). The expansions of cultivated and built-up regions at the expense of forest and shrublands has been affected by fast population growth and rising agricultural land demand (Eva *et al*., 2024; Siraj *et al*., 2023). These changes have reduced the natural water retention capacity, increased surface runoff, and accelerated soil erosion. Subsequently, the long-term viability of water supplies and ecosystem services within the watershed are threatened.

Numerous studies have investigated the effects of climate change and/or LULC change on watershed hydrology in Ethiopia. However, their separate and combined consequences were not evaluated using advanced hydrological models and next-generation climate projections. Most previous studies relied on earlier generations of climate models the Coupled Model Intercomparison Project Phase five

(CMIP5), which considered a limited number of climate scenarios, or assessed LULC and climate change separately. As a result, they overlooked the combined effects of these drivers on the watershed hydrology. Moreover, studies that integrate future LULC simulations, CMIP6 climate projections, and the recently restructured SWAT+ model remain limited in Ethiopian watersheds, especially in data-scarce semi-arid watersheds like the Dawe watershed.

Advances in spatial modeling and climate science provide an opportunity to address these limitations. The Cellular Automata-Markov (CA-Markov) model has demonstrated strong capability in simulating future LULC changes by capturing both temporal trends and spatial allocation patterns derived from historical satellite observations (Atulley, 2023; Semegnew *et al*., 2021). Similarly, the latest CMIP6 provides an improved representation of future climate variability and extremes under different projection scenarios compared with previous generations of Global Climate Models (GCMs) (Gebisa and Dibaba, 2024; Yilmaz *et al*., 2024). These variables are used as a robust input for hydrological simulations. These methods allow for thorough evaluation of future watershed responses under various land use and climate change scenarios when incorporated into hydrological models like SWAT+.

The purpose of this study was to evaluate the separate and combined impacts of future LULC change and climate change on the hydrological processes of the Dawe watershed, Ethiopia. Specifically, future LULC change patterns were simulated using the CA-Markov model; climate projections were derived from an ensemble of six CMIP6 GCMs under Shared Socioeconomic Pathways (SSP) SSP2–4.5 and SSP5–8.5 scenarios; and watershed hydrological responses were evaluated using the SWAT+ model. By integrating state-of-the-art land use modeling, future climate projections, and advanced hydrological simulation, this paper offers a comprehensive evaluation of potential water balance dynamics and generates scientific evidence to help sustainable management of watershed, climate change adaptation, and water security planning in semi-arid regions facing similar challenges.

Materials and Methods

Description of the Study Area

The study was conducted in the Dawe watershed, located in the northeast WSRB, Ethiopia. Geographically, it is situated between 9°13.5’ and 9°28.5' N and 41°42’ and 41°53’ E (Fig. 1). Its elevation ranges from 1695–3313 m above sea level, with the western part being mountainous and the eastern part being flat, predominantly agricultural land. The majority of the watershed is a sub-humid agro-ecological zone with an average yearly precipitation of 833 mm. Fig. 2 shows that the mean yearly high and low temperatures were 24.14°C and 10.99°C, respectively. The watershed has a low drainage density (0.55 km/km²), which is the ratio of the sum of all stream lengths (202.133 km) to the watershed area (368.94 km²). Lower drainage density indicates higher infiltration capacity, low runoff generation, and greater potential for groundwater recharge.

The watershed is distinguished by a mixed farming system that combines the production of livestock with crop cultivation (Zeleke *et al*., 2021). Agriculture is the dominant LULC type, followed by shrub land, with farmland covering more than 80% of the watershed. Soil and water conservation practices, including contour farming, soil bunds, and strip cropping (e.g., khat or coffee intercropped with sorghum, maize, or vegetables), are widely practiced (Roba *et al*., 2021). The predominant soil types are Rendzic Leptosols, Chromic Luvisols, Eutric Leptosols, and Humic Nitisols (Fig. 3).

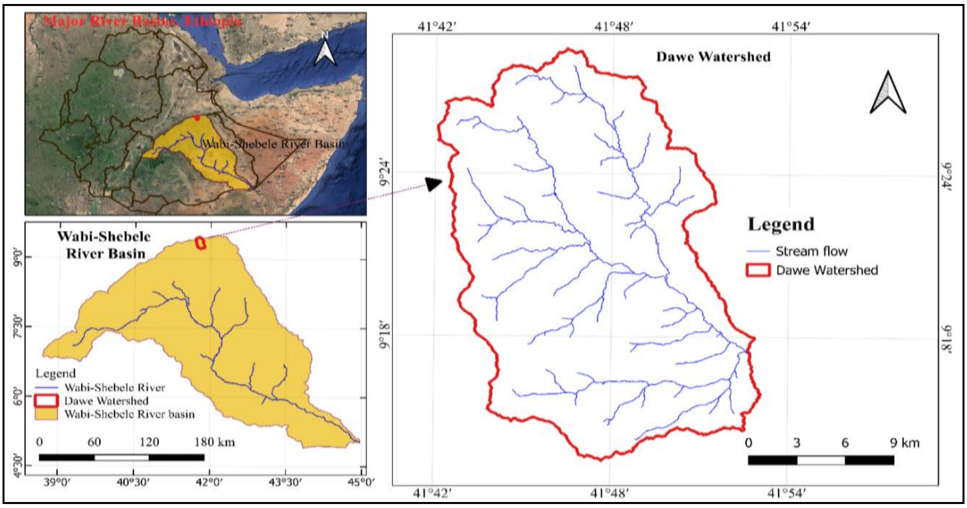

Figure 1. Location of the Dawe watershed in the northeast of the Wabi-Shebelle River basin.

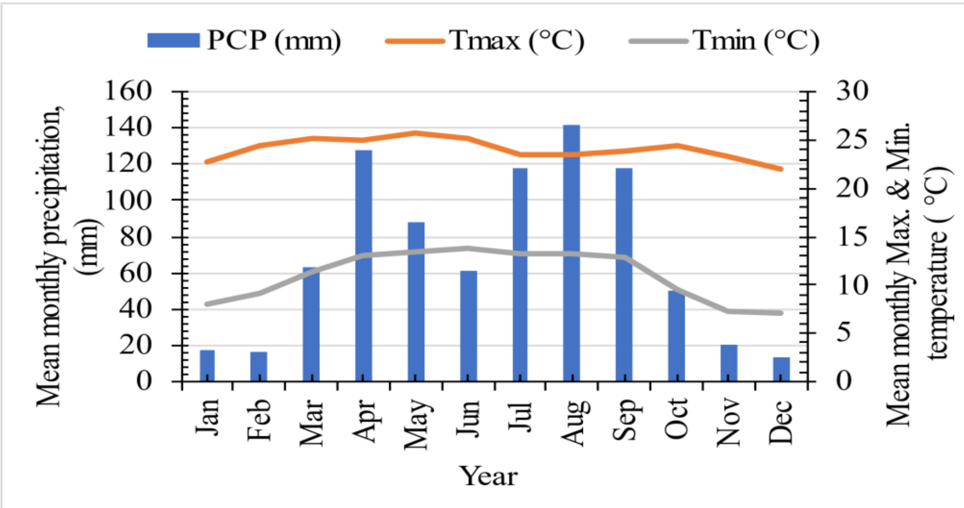

Figure 2. Historical monthly precipitation (mm), maximum, and minimum temperature (°C)

Database

Geospatial and hydrometeorological data

Landsat imageries (Table 1) (https://glovis.usgs.gov), DEM (https://search.earthdata.nasa.gov/), street network (https://www.openstreetmap.org/), stream network (derived from the DEM in SWAT+), and city center were used for LULC classification and prediction. Fig. 3 shows the DEM, soil (Harmonized World Soil Database), and LULC maps of the Dawe watershed. Meteorological (1988–2013) (Table 2) and hydrological data (1997–2013) were obtained from the Ethiopian Meteorology Institute (EMI) and Ministry of Water and Energy (MoWE) of Ethiopia, respectively.

Table 1. Landsat images and their characteristics, where MSS (Multispectral Scanner), ETM+ (Enhanced Thematic Mapper Plus), OLI (Operational Land Imager), and TIRS (the Thermal Infrared Sensor).

Product	Sensor	Acquisition Date (yyyy/mm/dd)	Path/Row	Resolution (m)	Day/night
Landsat 3	MSS	1985/01/20 1985/01/20	166/54,55	30	Day
Landsat 7	ETM+	2000/12/23 2000/12/07	166/54,55	30	Day
Landsat 8	OLI/TIRS	2022/01/26	166/54,55	30	Day

Sources: (https://glovis.usgs.gov)

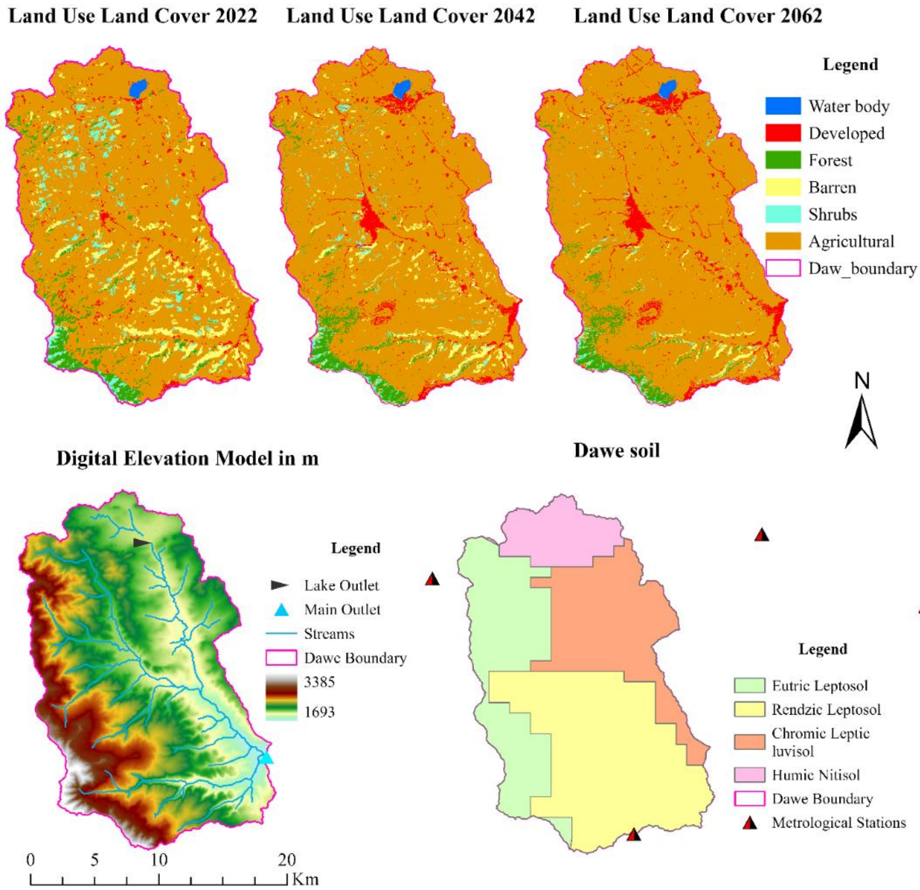

Figure 3. Digital elevation model, soils, LULC maps, and the meteorological station of the Dawe watershed.

Table 2. Meteorological stations and their geographic locations

ID	Station name	Latitude (decimal degree)	Longitude (decimal degrees)	Elevation (m)
1	Haramaya	9.40	42.03	2020
2	Dengego	9.45	41.92	2078
3	Harar	9.31	42.09	1977
4	Kullubi	9.42	41.68	2436

Climate model data

The ensemble of six CMIP6 GCMs' data for SSP2–4.5 and SSP5–8.5 (Table 3) for the period 2024–2085 was used for the simulation of hydrological data. The models were chosen based on the accessibility of the required variables (pr, tasmax, tasmin) and their capacity to reproduce Ethiopia in East African monsoon dynamics and seasonal rainfall patterns (Berhanu *et al*., 2023; Omay *et al*., 2023; Seifu and Eshetu, 2024). The SSP2–4.5 (moderate emissions) and SSP5–8.5 (fossil fuel-driven high-emissions) pathways were used because they represent contrasting yet widely used climate futures, thereby capturing a broad range of potential climate outcomes.

Table 3. Description of climate models for SSP2-4.5 and SSP5-8.5 emission scenarios

Model	Description	Institution	Spatial Resolution
ACCESS-CM2	Australian Community Climate and Earth System Simulator Coupled Model v2	CSIRO/Bureau of Meteorology	1° x 1°
CMCC-ESM2	Euro-Mediterranean Center on Climate Change Earth System Model v2	CMCC, Italy	1.875° x 1.875°
GFDL-ESM4	Geophysical Fluid Dynamics Laboratory Earth System Model Version 4	NOAA/GFDL, USA	1° x 1°
MPI-ESM1-2-LR	Max Planck Institute Earth System Model v1.2 Low Resolution	Max Planck Institute, Germany	1.875° x 1.875°
MRI-ESM2-0	Meteorological Research Institute Earth System Model v2.0	MRI, Japan	1.4° x 1.4°
NorESM2-MM	Norwegian Earth System Model v2 Medium Resolution	Norwegian Climate Centre (NCC)	2° x 2°

Source: https://cds.climate.copernicus.eu.

Bias Correction and Statistical Evaluation

Bias in GCM-simulated precipitation and temperature was corrected using the bias-correction algorithms implemented in the CMhyd (Rathjens *et al*., 2016). CMhyd is the most frequently used bias correction technique for analyzing how climate change affects water resources at the watershed level (Seifu and Eshetu, 2024).

The Linear–scaling approach was used in the bias correction. It assumes that the historical model–observation bias remains sufficiently stable for the correction factors to be applicable to future simulations. The observed station data were used as the reference dataset. Monthly correction factors were derived from the past period and applied separately to precipitation and temperature. A multiplicative correction was used for precipitation, while an additive correction was applied to temperature. Using Root Mean Squared Error (RMSE), Mean Absolute Error (MAE), and PBIAS, the efficacy of the bias correction was assessed by comparing raw and bias-corrected simulations with observations for each station–GCM combination.

Methods

General Framework

Fig. 4 presents the conceptual framework of the study. It integrates remote sensing-based LULC analysis, hydrological modeling, and climate modeling to assess how the hydrology of the Dawe watershed will be affected by potential change in LULC and climate.

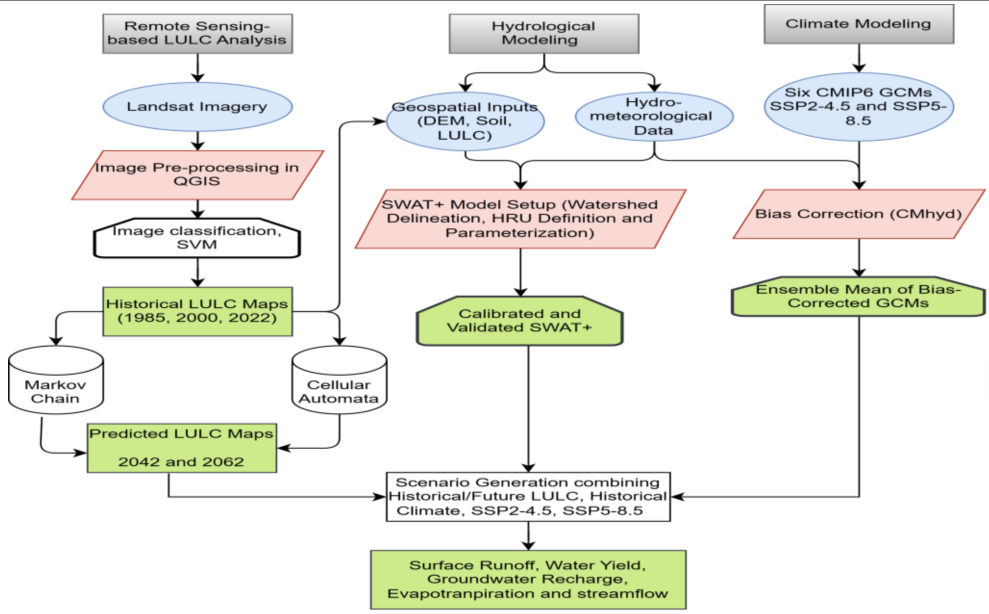

Figure 4. A framework to estimate watershed hydrology by integrating LULC prediction, SWAT+ hydrological modeling, and an ensemble of six CMIP6 GCMs to estimate watershed hydrology. Blue represents input datasets, pink denotes data processing and model setup, white indicates analytical/modeling processes, and green represents intermediate and final outputs.

Land Use/Land Cover Classification and Prediction

The historical LULC was classified from Landsat imageries (2000 and 2022) using a Support Vector Machine (SVM) algorithm in ArcGIS Pro. The error matrix was used to generate the overall accuracy (OA), which represents the overall classification accuracy across all LULC classes (Congalton and Green, 2019). The land use classification by chance was taken into account using Cohen's Kappa coefficient (K), a robust nonparametric statistical measure (Rwanga and Ndambuki, 2017). The kappa value varies from –1 to 1. A kappa of –1, 0, and 1 denotes disagreement, agreement by chance, and perfect agreement, respectively. The SVM was chosen because of its track record of outperforming other machine learning (ML) algorithms in terms of overall classification accuracy (Siraj *et al.*, 2023).

A CA-Markov model within the Land Change Modeler (LCM) in Idris TerrSet was used to predict the LULC of 2042 and 2062. The CA-Markov model was used to project future LULC based on historical transition patterns. It integrates the temporal transition probabilities of the Markov chain with the spatial allocation capabilities of CA to simulate future LULC patterns (Gebresellase *et al.*, 2023).

Hydrological Model

The SWAT model, a large-scale basin model, is most commonly used globally due to ease of obtaining input, high computational efficiency, its capability of long-term watershed simulation, and its being in the public domain (Arnold *et al.*, 1998). SWAT+, a completely redesigned version of SWAT, a powerful distributed hydrological model with several uses, was employed in this investigation (Bieger *et al.*, 2017).

Model Setup

The Dawe watershed was divided into 25 sub-basins, 73 landscape units (LSUs), and 1631 hydrological response units (HRUs) using QSWAT+ following its delineation. The Muskingum method was used to simulate monthly stream flow, and Penman–Monteith was used for PET estimation (Bieger *et al*., 2017).

Model parameter sensitivity analysis

The SWAT+ Toolbox was employed to perform the sensitivity of model parameters, and the model calibration and validation. Due to the existence of hundreds of parameters describing hydrological, soil, land-use and management processes 18 commonly used were chosen through a combination of literature information and the researchers' expertise. The impact of these parameters on the model's results was assessed utilizing Random Balance Designs–Fourier Amplitude Sensitivity Test (RBD-FAST) within the SWAT+ Toolbox version. RBD-FAST is a comprehensive sensitivity analysis method that employs the Fourier amplitude sensitivity test through a random balance design strategy (Xiang *et al*., 2022). The parameters were ranked depending on how they affected the model's simulation after the sensitivity study was finished. The parameter with the greatest impact was assigned the first rank, indicating its significant effect on the model results, while the parameter with the lowest impact was ranked last. Subsequently, the top 12 parameters from the sensitivity ranking were selected for the tasting and verifying the model.

Calibration and Validation

The SWAT+ model development covered the period from 1998–2013. The model was calibrated for the period from 2000 to 2008; the first two years were used for model warm-up. Then, the model was validated for the period from 2009–2013. Automatic calibration was performed using the 'Calibration by Latin-hypercube Sampling Iterations (CALSI)' algorithm. Based on the value of the objective function, the alignment between the observed and simulated stream flow hydrograph, and the water balance ratios, the model parameters were manually calibrated (Arnold *et al*., 2012).

Nash-Sutcliffe Efficiency (NSE) (Nash and Sutcliffe, 1970), Kling-Gupta Efficiency (KGE), PBIAS, and coefficient of determination (R^2) (Arnold *et al*., 2012) were used to assess the hydrological model performance during calibration and validation. The NSE shows how well the 1:1 line fits the plots of the simulated and observed stream flow data. The NSE measures how well the two data values agree. It ranges from $-\infty$ to 1, with a value closer to 1, demonstrating better model performance. NSE of 0 shows poor model performance, which is no better than the observed mean, while values less than 0 indicate that its performance is worse than the observed mean.

The average tendency of the simulated data to match the observed data was compared using PBIAS. The ideal PBIAS value is zero. For stream flow model simulations, NSE > 0.50 and PBIAS < ±25% were deemed acceptable (Moriasi *et al*., 2007). R^2 is the degree to which the simulated and observed values have a linear relationship. Greater model performance is shown by higher values on the R^2 scale, which ranges from 0 to 1.

Furthermore, KGE was used, which combines correlation coefficient, variability ratio, and bias ratio to create a single measure of model performance. The constraints of NSE and R^2 were overcome by KGE's capacity to replicate the timing and variability of the observed data (Gupta *et al*., 2009). The range of KGE is $-\infty$ to 1, where 1 denotes perfect agreement and more than 0.75 is being considered acceptable.

LULC and climate change impact assessment

This study used a comparative scenario-based method to measure the separate and combined impacts of LULC dynamics and climate changes on hydrological components (SR, GWR, WY, and ET). The combination of two climate projections (SSP2–4.5 and SSP5–8.5) and two predicted LULC maps (LULC 2042 and 2062) was considered across two time periods: mid-century (2024–2055) and late-century (2056–2085). Nine scenarios, spanning from S0–S8, were developed, as summarized in Table 4.

Two climate projections were selected because these emission scenarios capture a broad range of plausible climate futures, from intermediate to worst-case conditions. SSP2–4.5 corresponds to a moderate emission trajectory, assuming sustainable development and partial mitigation, while SSP5–8.5, on the other hand, represents a development route with high emissions and a strong reliance on fossil fuels (Riahi *et al.*, 2017). The LULC map of 2022 was used as a reference, while the LULC 2042 and LULC 2062 projections were used to capture the future land cover dynamics within 2022–2055 and 2056–2085, respectively. The selected time horizons were aligned with the standard climate assessment periods recommended by the IPCC. This makes it possible to assess long-term hydrological threats and short- to mid-term adaptation requirements.

The impact of LULC alteration on hydrological components was assessed using a differential scenario-based approach. In hydrological impact assessments, this method is frequently employed to determine the overall impact of LULC change under stationary climate assumptions. We recognize that this assumption does not take into consideration possible feedbacks (e.g., LULC-induced changes in local evapotranspiration altering regional rainfall patterns). However, considering the limits of the SWAT+ framework with respect to independent LULC-only simulations under future climatic forcing, the differential approach is still suitable for this investigation. Therefore, rather than focusing on absolute attribution, the data are interpreted cautiously, emphasizing the direction and relative size of LULC-driven changes.

Table 4. Summary of the scenario matrix. "Mid" stands for mid-century (2024–2055), and "Late" for late-century (2056–2085).

Scenario	LULC	Climate
S0	2022	Baseline
S1	2022	SSP2-4.5 Mid
S2	2022	SSP2-4.5 Late
S3	2022	SSP5-8.5 Mid
S4	2022	SSP5-8.5 Late
S5	2042	SSP2-4.5 Mid
S6	2042	SSP5-8.5 Mid
S7	2062	SSP2-4.5 Late
S8	2062	SSP5-8.5 Late

Source: Own Study

RESULTS

Projected LULC Change

The CA-Markov model in Idrisi software was employed to predict the LULC maps for 2042 and 2062 (Table 5). The model's ability to predict LULC change was evaluated using three Kappa statistics: Klocation (0.82), Kstandard (0.75), and Kno (0.84). OA of 89% and κ of 0.87, the historical classification reveals a high degree of agreement between the classified map and the reference material. PA ranging from 82.0% to 96.5% and UA ranging from 86.5% to 92.5% (Table 6) demonstrate strong classification performance.

Table 5. Present and predicted LULC of the northeast WSRB. LULC 2022 is based on Landsat 8 image classification using a support vector machine (SVM).

LULC	Area (km²)			Change in %		
	2022	2042	2062	2042-2022	2062-2042	2062-2022
Water	6.8	5.31	4.06	-21.90	-23.50	-40.25

Developed	137.8	406.93	918.18	195.31	125.63	566.31
Forest	329.8	228.83	197.44	-30.62	-13.72	-40.13
Barren	2853.5	2898.71	2992.33	1.58	3.23	4.87
Shrubs	7615.9	7079.92	6111.63	-7.04	-13.68	-19.75
Agriculture	3883.8	4208.20	4603.70	8.35	9.40	18.54

Table 6. Confusion matrix showing the accuracy assessment of historical land use/land cover classification.

LULCC	Water	Developed	Forest	Barren	Shrubs	Agriculture	Total	UA
Water	74	0	3.00	0.50	1.50	1.00	80	0.925
Developed	0	80	0.50	6.00	0.50	3.50	90	0.885
Forest	4.5	0	84.50	1.00	6.00	1.50	97	0.865
Barren	0.5	2	0.00	92.50	3.50	4.00	102	0.895
Shrubs	1.5	1	9.00	9.00	173	3.00	196	0.88
Agriculture	0.5	0	2.00	3.50	9	113.50	128	0.885
Total	81	83	99.00	112.50	193.5	126.50	693	713
PA	0.915	0.97	0.86	0.82	0.89	0.90		
Kappa coefficient = 0.87 and Overall accuracy = 0.89								

where PA = Producer's Accuracy, UA = User's Accuracy.

Climate Model Bias Correction

The bias-correction results (Table 7) show substantial improvements in the CMIP6 simulations. For rainfall, RMSE decreased by 33.1%, MAE by 11.9%, and PBIAS by 87.6%. On the other hand, Tmax RMSE and MAE decreased by 48.7% and 57.9%, while Tmin showed reductions of 66.8% and 73.7%, respectively. Absolute systematic bias was reduced by 99.3% for Tmax and 97.9% for Tmin. Aggregates of post-bias-correction by stations and GCMs are given in Table 7, 8 & 9.

Table 7. Post-bias correction performance aggregated by station (mean and range across all six GCMs).

Station	Variable	RMSE (Mean ± Range)	MAE (Mean ± Range)	PBIAS (Mean ± Range)
Dengego	Precip	7.94 (7.37 – 8.71)	3.33 (2.83 – 3.80)	-2.73 (-8.27 – 1.38)
	Tmax	3.56 (2.55 – 4.16)	2.34 (2.00 – 2.80)	-0.10 (-0.92 – 0.17)
	Tmin	3.80 (3.56 – 4.62)	2.31 (2.01 – 3.49)	3.59 (0.00 – 19.77)
Haramaya	Precip	7.66 (7.08 – 8.45)	3.18 (2.83 – 3.79)	-2.86 (-8.55 – 0.00)
	Tmax	2.68 (2.34 – 3.17)	2.10 (1.84 – 2.48)	0.97 (0.00 – 5.84)
	Tmin	3.63 (3.41 – 4.29)	2.75 (2.53 – 3.06)	0.01 (0.00 – 0.02)
Harar	Precip	7.38 (6.81 – 8.20)	3.10 (2.81 – 3.70)	-3.18 (-10.89 – 0.00)
	Tmax	3.07 (2.59 – 4.01)	2.24 (1.91 – 2.70)	0.79 (-0.01 – 4.80)
	Tmin	2.45 (2.29 – 2.47)	1.79 (1.68 – 1.92)	0.00 (-0.01 – 0.00)
Kulubi	Precip	8.73 (8.31 – 9.36)	3.60 (3.40 – 4.14)	-4.30 (-12.09 – 0.34)
	Tmax	3.98 (3.61 – 4.52)	2.28 (1.98 – 2.86)	-0.85 (-8.90 – 0.35)
	Tmin	2.34 (1.88 – 3.33)	1.82 (1.41 – 2.72)	-2.28 (-18.53 – 0.00)

Table 8. Post-bias correction performance aggregated by GCM (mean across all four stations).

GCM	Precip RMSE	Precip PBIAS	Tmax RMSE	Tmax PBIAS	Tmin RMSE	Tmin PBIAS
ACCESS-CM2	7.88	-0.74	3.05	0.13	2.98	0.11
GFDL-ESM4	8.65	0.13	3.30	0.13	3.08	0.11
MPI-ESM1-2-LR	7.39	-9.95	3.65	2.79	3.29	0.72
MRI-ESM2-0	8.30	-0.01	3.78	0.00	2.86	0.00
NESM3	7.39	-9.43	3.01	-1.74	3.15	-4.63
NorESM2-MM	7.92	0.00	2.69	-0.14	3.23	4.94

Table 9. Summary of bias-correction performance for rainfall and temperature maximum (T_{max}) and minimum (T_{min}) across all stations and GCMs, showing RMSE, MAE, and PBIAS before (Raw) and after (BC) correction.

Variable	RMSE Raw → BC	MAE Raw → BC	PBIAS Raw → BC
Rainfall	11.74 → 7.85	3.95 → 3.48	−33.73 → −4.17%
Tmax	6.31 → 3.24	5.18 → 2.18	20.93 → 0.14%
Tmin	9.30 → 3.09	8.39 → 2.21	75.92 → 1.63%

Climate Change Trend

The projected climate data from the six-GCM ensemble from CMIP6 projects a significant warming trend by the late 21st century (Fig. 5). The average yearly temperature under the SSP2–4.5 and SSP5–8.5 scenarios is predicted to rise by 2.54°C and 3.44°C, respectively, over the baseline period (1988–2013).

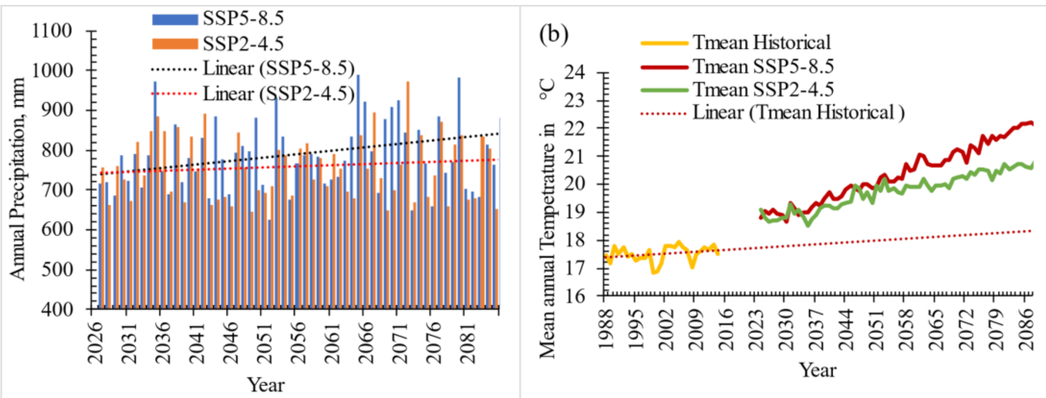

Figure 5. Projected annual precipitation (a) and average annual temperature (b) for the 2024–2085 SSP2–4.5 and SSP5–8.5 scenarios.

Calibrated and Validated QSWAT+

The calibrated parameters with their range of values, sensitivity order, and auto- and manual-fitted values are listed in Table 10. The sensitivity analysis showed that CN2 was most sensitive, followed by the soil evaporation compensation factor (ESCO) and percolation coefficient (PERCO). This implies that land use and soil type are the most important variables controlling the water flow in the area.

Table 10. Sensitivity analysis and calibrated values of key hydrological parameters showing their relative influence on model performance, allowable ranges, parameter adjustments, and final fitted values.

Parameters	**Descriptions**	**Value Range**	**Sensitivity order**	**Adjustment value**	**Fitted Value**
p_CN2	SCS curve number for moisture condition II	±20	1.535	3.652	78.776
r_ESCO	Soil Evaporation Compensation Factor	0 - 1	0.277	0.206	0.206
r_PERCO	Percolation Coefficient	0 - 1	0.228	0.684	0.684
p_BD	Soil Bulk Density	±20	0.198	11.448	1.337
r_REVAP_CO	Groundwater "revap" coefficient	0.02 – 0.2	0.039	0.115	0.115
p_AWC	Available water capacity of the soil layer	±10	0.007	5.292	0.097
p_SURLAG	Surface Runoff Lag Coefficient	±30	0.005	4.007	13.729
p_FLO_MIN	Threshold depth for groundwater flow	0 - 20	0.0003	0.407	0.973
r_ALPHA	Baseflow Alpha Factor	0.01-0.9	-0.0013	0.583	0.583
p_K	Saturated Hydraulic Conductivity	±10	-0.007	13.981	23.047
r_CN3_SWF	Soil Water Factor for Curve Number III	0 – 1	-0.079	0.189	0.189
r_CANMX	Maximum Canopy Storage	1 - 100	-0.118	17.728	17.728

p represents the percent of change of the default value of parameters, and r represents changes of parameters in which the existing value is replaced by the new value. Negative sensitivity values for K, CN3_SWF, and CANMX indicate inverse relationships with stream flow.

The SWAT+ demonstrated a strong association between the simulated and observed streamflow. as indicated by the KGE, NSE, R^2, and PBIAS values during both the calibration and validation periods. The results show that the SWAT+ model is trustworthy for upcoming evaluations of the effects of climate change (Fig. 6).

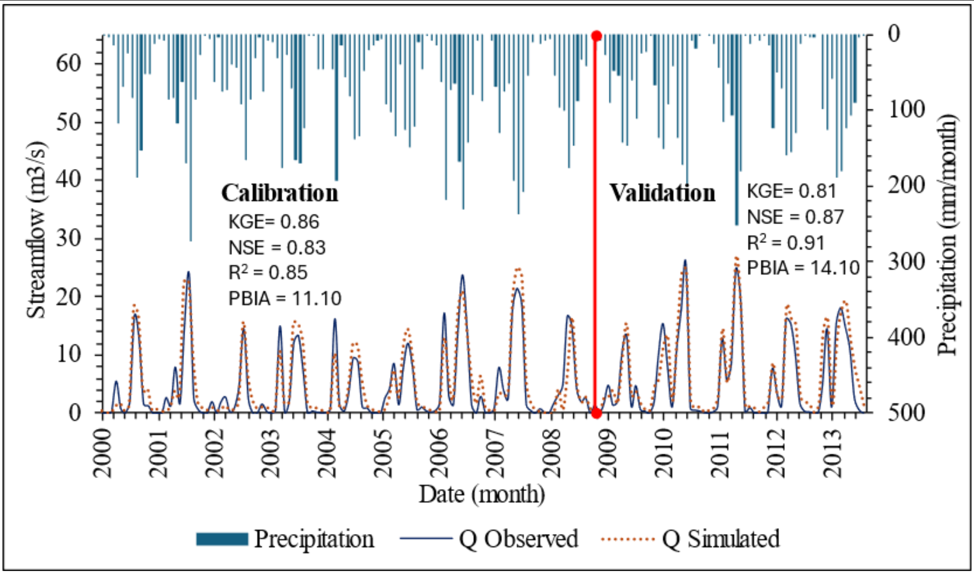

Figure 6. Hydrograph of measured and simulated streamflow (Q) during testing (2000–2008) and verification (2009–2013) at the Dawe watershed.

Impact of LULC and Climate Change on Hydrological Components

Climate change impacts

Table 11 reveals the effects of climate change on water balance elements like SR, GWR, WY, and ET. The individual impacts of climate change under both SSP2–4.5 and SSP5–8.5 with constant LULC (2022) are represented in S1–S4. The projected WY and SR will decline by 17.16% and 21.75% in the late century (S2) and 19.10% and 23.22% in the mid-century (S1) under SSP2–4.5, respectively. Groundwater recharge's response to climate change showed inconsistency under different scenarios. GWR under S1 and S2 increased by 7.90% and 10.07%, respectively, whereas under S4, it decreased by 19.82%. In contrast, ET consistently increased (by 13.00 to 23.4%) under all scenarios (S1 to S4) in response to climate change.

Table 11. The simulated annual mean hydrological components

Scenario	SR	ΔSR %	GWR	ΔGWR %	WY	ΔWY%	ET	ΔET %
So	134.00	-	73.94	-	381.62	-	602.43	-
S1	108.40	-19.10	79.38	7.36	293.02	-23.22	682.96	13.37
S2	111.00	-17.16	81.38	10.07	299.31	-21.57	702.8	16.66
S3	116.30	-13.21	78.66	6.38	313.49	-17.85	703.53	16.78
S4	93.77	-30.02	59.29	-19.82	276.69	-27.50	744.41	23.57
S5	109.20	-18.51	77.53	4.85	295.11	-22.67	680.66	12.99
S6	117.10	-12.61	76.80	3.87	315.67	-17.28	703.09	16.71
S7	92.77	-30.77	59.29	-19.82	302.23	-20.8	700.19	16.23
S8	89.95	-32.87	56.78	-23.21	249.95	-34.5	743.76	23.46

Combined Impacts of LULC and Climate Change

The combined impact of future LULC and climate change scenarios altered all major hydrological components (Table 9). Compared with the baseline, surface runoff decreased by 12.61–32.87%, groundwater recharge ranged from a 4.85% increase to a 23.21% decrease, water yield declined by 20.80–34.50%, and evapotranspiration increased by 12.99–23.46%. The largest changes were observed under Scenario S8 (2062 LULC + SSP5–8.5), which recorded a 32.87% reduction in surface runoff, a 23.21% reduction in groundwater recharge, a 34.50% reduction in water yield, and a 23.46% increase in evapotranspiration.

Fig. 7 illustrates the effects of both LULC and climate changes on annual mean stream flow under the baseline scenario (S0) and late-century scenario (S8). Under the S8 scenario, stream flow reductions were widespread, with the highest flows dropping from 3.45–4.45 m³/s in the baseline scenario to 1.97–2.51 m³/s, indicating reduced base flow contributions and diminished upstream water availability. These declines threaten household water supplies, irrigation potential, ecological water needs, and the sustainability of dry-season flows along the mainstream.

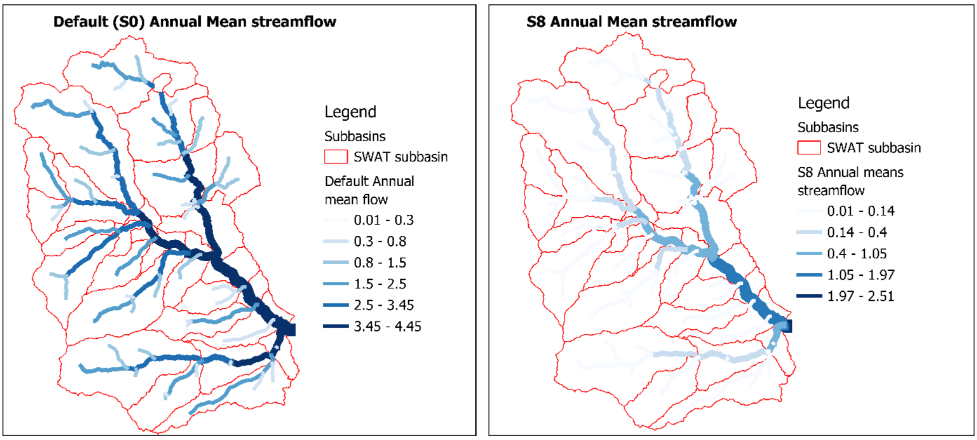

Figure 7. Spatial comparison between the annual average streamflow for S8 and S0 scenarios in response to the LULC and climate changes.

LULC impacts

To determine the incremental impacts of LULC dynamics on hydrological components, the combined scenarios' effects were compared to their respective climate impact equivalents. For instance, the SR difference between S5 and S1 is minimal (–18.51% vs. –19.10%), which may indicate that in SSP2–4.5, LULC has limited additional influence. However, the GWR dropped from +7.36% (S1) to +4.85% (S5), suggesting that future LULC may limit infiltration slightly because of the expansion of developed and barren land. Similar to this, WY differences between S6 and S3 in SSP5 are minimal (–17.28% vs. –17.85%), but ET is still substantial and dominated by warming.

In the late-century scenarios (S7 and S8), the combined impact is more apparent. For example, SR decreased from –30.02% in S4 (climate only) to –32.87% in S8 (with 2062 LULC), and WY decreased further (–27.5% to –34.5%). This implies that the drying effect of extreme climate change is amplified by landscape degradation.

DISCUSSIONS

Impacts of Projected LULC Dynamics on Hydrological Processes

The predicted LULC changes in the Dawe watershed for 2042 and 2062 indicate substantial transformation, marked by swift growth of the urban area and agricultural land. These changes significantly affect hydrological processes by modifying infiltration, runoff generation, and evapotranspiration. The expansion of built-up area increases impermeable surfaces, which raises the risk of flash flooding, soil erosion, and sedimentation. Similarly, because of decreased interception and soil water retention, the growth of agricultural land at the cost of natural vegetation tends to increase SR and decrease GWR (Aragaw and Kura, 2024; Lukas *et al*., 2025).

Nevertheless, the Dawe watershed is predominantly agricultural, with farmland encompassing more than 80% of the total land area. On the farmlands, conservation techniques for soil and water (Fig. 8), like contour farming, bunds, and strip cropping (khat or coffee and sorghum or maize or vegetables), might have contributed to the reduction of surface runoff and increase in GWR and ET, particularly under S1 and S2. This result is in line with earlier research. showing that soil and water conservation interventions can substantially modify watershed hydrological responses by improving soil moisture retention and reducing overland flow (Woldemariam *et al*., 2018; Yaekob *et al*., 2022).

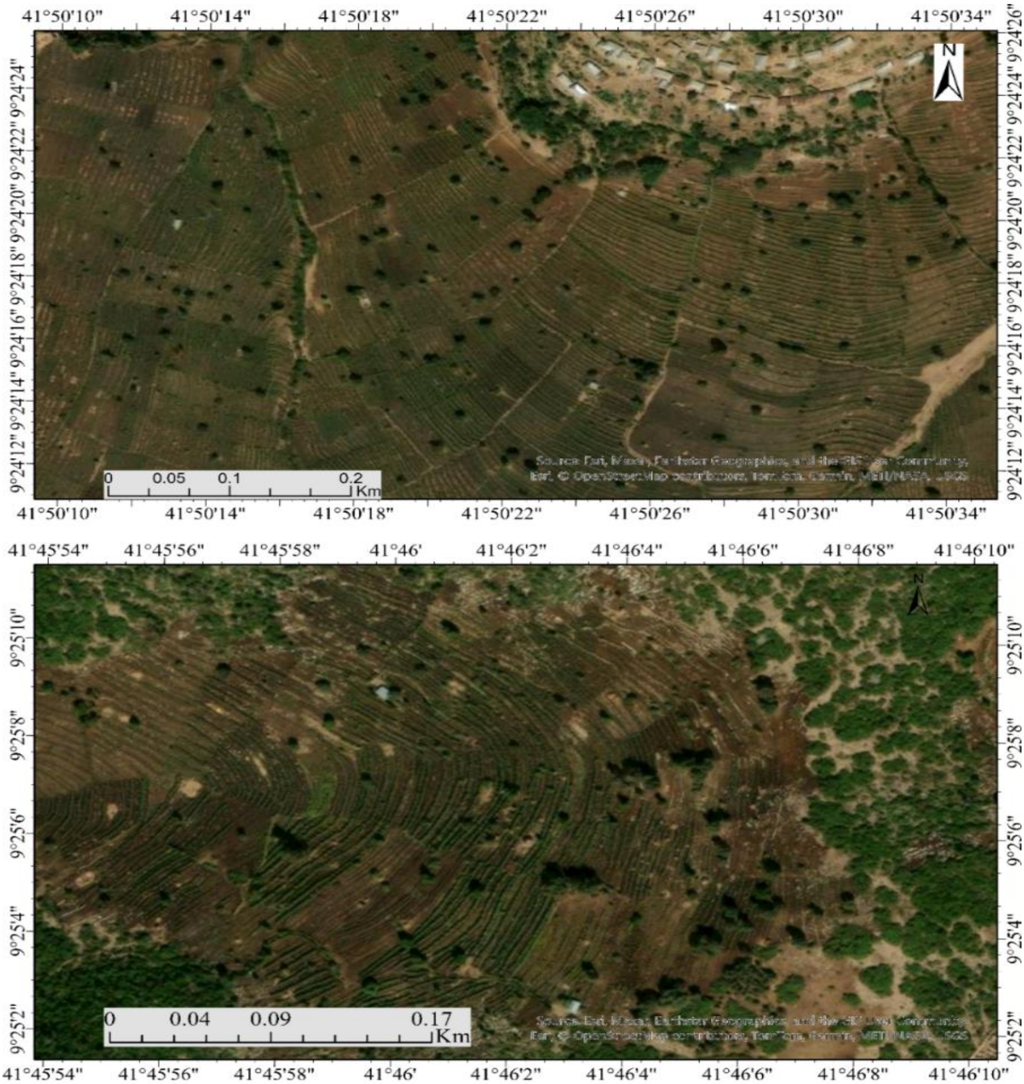

Figure 8. Images of soil water conservation practices on the cultivated area (image source: Google Earth Pro, accessed on July 23, 2025).

Projected Climate Change Patterns in the Dawe Watershed

The findings of this investigation align with the projected global mean average warming rate, which projected average surface temperature will exceed 2–4°C under intermediate to high-emission pathways (IPCC, 2023a). The projected warming is also comparable to regional findings by Tikuye *et al.* (2024), who reported an ensemble temperature increase of 4.9°C in the Upper Blue Nile Basin under RCP8.5 by the end of the century, consistently indicating substantial warming under high-emission scenarios. The slight variation in projected warming can be attributed to differences in emission scenarios (CMIP6 SSPs versus CMIP5 RCPs), climate models, bias-correction methods, and the distinct geographical and topographic characteristics of the study regions. Moreover, these findings agree with regional projections for East Africa, which consistently indicate accelerated warming and increasing exposure to extreme heat (Babaousmail e*t al*., 2024; Choi *et al*., 2023).

Although mean annual precipitation is projected to increase slightly, substantial interannual variability, particularly under the SSP5–8.5 scenario, introduces considerable uncertainty in future water availability. These results are consistent with recent climate studies conducted in Ethiopia, which show strong and steady warming trends but geographically and temporally varied precipitation responses to climate change (Feleke *et al*., 2025). Increased precipitation does not always equate to improved water security. Droughts and floods may become more likely if rainfall patterns shift and precipitation events become more extreme. Future hydrological regimes will therefore probably be more erratic, which will present serious difficulties for managing water supplies, increasing agricultural output, and adapting to climate change.

Combined Impacts on Watershed Hydrological Processes

The findings showed rising ET and falling SR, WY, and GWR, which indicate a drop in the watershed's total water supply and a rise in atmospheric water demand. Similar ET increases have been reported in several Ethiopian watersheds. For instance, Mechal and Bayisa (2025) and Balcha *et al.* (2023) concluded that future warming substantially increased ET and altered basin water balance components in the Central Rift Valley Lakes Basin. Daniel (2023) and Truneh *et al.* (2024) also reported that agricultural expansion and urbanization enhanced ET by increasing atmospheric water demand and modifying land surface characteristics. However, contrasting findings from some studies indicate that ET responses remain highly dependent on local agro-ecological conditions, land management practices, and climate variability (Ayalew *et al.*, 2024).

The projected declines in SR and WY align with findings from major Ethiopian basins such as the Wabi-Shebelle and Upper Blue Nile basins. These studies revealed that the combined impact of LULC and climate change reduces stream flow and alters flow duration characteristics, particularly low flows (Fita and Abate, 2022). By contrast, studies in neighbouring watersheds have demonstrated that deforestation and cropland expansion may locally increase runoff and stream flow due to reduced infiltration and interception (Abdule *et al*., 2023; Chanie, 2024). These conflicting results highlight how local watershed management, land-cover dynamics, and climate forcing interact to significantly impact hydrological responses throughout watersheds.

It is anticipated that future LULC and climate change scenarios will drastically lower GWR, making shallow groundwater resources more vulnerable to drought and intensifying competition. This finding is consistent with several studies conducted across Ethiopia. For instance, Chuko and Abdissa (2023) and Woldu *et al*. (2024) reported that conversion of natural vegetation to agricultural land and built-up area reduces recharge through impaired infiltration and increased surface sealing. Although soil and water conservation measures and moderate climate shifts may locally buffer GWR (Tofu *et al*., 2023), the overall trajectory for the Dawe watershed indicates a net reduction in groundwater replenishment. Concurrent depletion of surface and groundwater resources may have detrimental effects on household water supplies, agricultural productivity, and ecosystem sustainability.

Conclusions and Recommendations

This study integrated the CA-Markov land-use change model, an ensemble of six CMIP6 GCMs, and the SWAT+ hydrological model to examine the effects of potential LULC and climate changes on the hydrological processes of the Dawe watershed. By integrating these complementary models, the study provides a comprehensive framework for evaluating watershed responses under change scenarios. The findings reveal the value of integrated assessments for supporting long-term water resource planning.

The results indicate that agricultural land and developed areas will continue to broaden, while forests and shrub lands will decline. These changes will be reinforced by rising temperatures. Consequently, the watershed hydrological regime will be substantially altered. Climate change was identified as the primary driver of future hydrological change, while LULC change further amplified its effects. Across all future scenarios, evapotranspiration increased, whereas water yield, surface runoff, and groundwater recharge declined. The SSP5-8.5 and 2062 LULC scenarios resulted in the greatest hydrological decline. This finding highlights the importance of considering the combined effects of land-use change and climate change on future water availability.

The findings suggest that sustainable water resource management should integrate climate adaptation with land-use planning rather than addressing these drivers independently. Protecting remaining forests, restoring degraded shrub lands, implementing soil and water conservation measures, and promoting agroforestry should be prioritized to enhance infiltration, groundwater recharge, and watershed resilience. Increasing the effectiveness of agricultural water use through water-saving irrigation technologies, rainwater harvesting, and drought-tolerant crop varieties will also be essential to reduce pressure on increasingly limited water resources.

Future research should improve integrated assessments by incorporating socioeconomic drivers of land-use change, coupling surface water and groundwater models (e.g., SWAT-MODFLOW). The cumulative downstream impacts across the Wabi-Shebelle River Basin need to be evaluated. Additionally, uncertainty analyses using multiple climate and hydrological models would also support the scientific basis for managing water resources in an adaptable and sustainable manner under future environmental changes.

Declarations

Competing interests: The authors have no competing interests to declare that are relevant to the content of this article.

Ethics and Consent to Participate declarations

|Not applicable

Funding

The study received funds from Haramaya University and Ethiopian Ministry of Education.

Data Availability Statement

The datasets generated and/or analyzed during the current study are available from the corresponding author on reasonable request.

Author contributions

All the authors contributed to the conceptualization and design of the study. The corresponding author, Birhanu Legesse Wakjira, acquired and analyzed the data and wrote the manuscript. The other authors, Asfaw Kebede Kassa, Awdenegest Moges, and Olkeba Tolessa Leta, critically revised and strengthened the overall manuscript.

Acknowledgments

I would like to express my gratitude to the Ethiopian Ministry of Education and Haramaya University for funding this research work. The majority of the materials and information utilized were gathered from the Ministry of Water and Energy and the National Meteorological Agency of Ethiopia and are gratefully acknowledged for granting access to the data.

References

Abdule, A. M., Muluneh, A. & Woldemichael, A. (2023). Impact of Climate and Land Use/Cover Changes on Streamflow in Yadot Watershed, Genale Dawa Basin, Ethiopia. *Air, Soil and Water Research*, 16. https://doi.org/10.1177/11786221231200106

Amsalu, S. (2019). Review on the Cause and Effects of Recurrent Drought on Ethiopian Agriculture Productivity. *International Journal of Horticulture, Agriculture and Food Science*, 3(5), 292–298. https://doi.org/10.22161/ijhaf.3.5.7

Aragaw, H. M., Goel, M. K. & Mishra, S. K. (2021). Hydrological Responses to Human-Induced Land Use/Land Cover Changes in the Gidabo River Basin, Ethiopia. *Hydrological Sciences Journal*, 66(4), 640–655. https://doi.org/10.1080/02626667.2021.1890328

Aragaw, H. M. & Kura, A. L. (2024). Hydrological Response to Land Use/Land Cover Changes in Ethiopian Basins: A Review. *Hydrological Sciences Journal*, 69(7), 986–996). https://doi.org/10.1080/02626667.2024.2349272.

Arnold, J. G., Moriasi, D. N., Gassman, P. W., Abbaspour, K. C., White, M. J., Srinivasan, R., Santhi, C., Harmel, R. D., Van Griensven, A., Van Liew, M. W., Kannan, N. & Jha, M. K. (2012). SWAT: Model Use, Calibration, and Validation. *Transactions of the ASABE*, 55(4), 1491–1508. https://doi.org/10.13031/2013.42259

Arnold, J. G., Srinivasan, R., Muttiah, R. S. & Williams, J. R. (1998). Large Area Hydrologic Modeling and Assessment — Part I: Model Development. *Journal of the American Water Resources Association*, 34(1), 73–89.

Atulley, J. A. (2023). Simulating future land cover change in the Tono catchment using the CA-Markov model. *Research Square*, https://doi.org/https://doi.org/10.21203/rs.3.rs-2401213/v1.

Ayalew, A. D., Wagner, P. D., Sahlu, D. & Fohrer, N. (2024). Unveiling hydrological dynamics in data-scarce regions: Experiences from the Ethiopian Rift Valley Lakes Basin. *Hydrology and Earth System Sciences*, 28(8), 1853–1872. https://doi.org/10.5194/hess-28-1853-2024

Ayalew, S. E. & Nigussie, T. A. (2023). Historical and projected land-use / land cover changes of the Welmel River Watershed, Genale Dawa Basin, Ethiopia. *Journal of Water and Land Development*, (58), 89–98. https://doi.org/10.24425/jwld.2023.146601

Babaousmail, H., Ayugi, B. O., Lim Kam Sian, K. T. C., Randriatsara, H. H. R. H. & Mumo, R. (2024). How Do CMIP6 HighResMIP Models Perform in Simulating Precipitation Extremes over East Africa? *Hydrology*, 11(7). https://doi.org/10.3390/hydrology11070106

Balcha, S. K., Awass, A. A., Hulluka, T. A., Bantider, A. & Ayele, G. T. (2023). Assessment of future climate change impact on water balance components in Central Rift Valley Lakes Basin, Ethiopia. *Journal of Water and Climate Change*, 14(1), 175–199. https://doi.org/10.2166/wcc.2022.249

Berhanu, D., Alamirew, T., Taye, M. T., Tibebe, D., Gebrehiwot, S. & Zeleke, G. (2023). Evaluation of CMIP6 models in reproducing observed rainfall over Ethiopia. *Journal of Water and Climate Change*, 14(8), 2583–2605. https://doi.org/10.2166/wcc.2023.502

Bieger, K., Arnold, J. G., Rathjens, H., White, M. J., Bosch, D. D., Allen, P. M., Volk, M. & Srinivasan, R. (2017). Introduction to SWAT+, A Completely Restructured Version of the Soil and Water Assessment Tool. *Journal of the American Water Resources Association*, 53(1), 115–130. https://doi.org/10.1111/1752-1688.12482

Bikeko, S. S. & Venkatesham, E. (2024). Land use land cover change as a casual factor for climate variability and trends in the Bilate Watershed, Ethiopia. *Environmental Monitoring and Assessment*, 196(12), 1250. https://doi.org/10.1007/s10661-024-13435-y

Birhan Getachew, T., Ray, R. L., Gebeyehu, K. & Teshome, M. (2024). Assessing the influence of land use/land cover dynamics and climate change on water resources in Upper Blue Nile, Ethiopia. *Journal of Water and Climate Change*, 15(9), 4745–4774. https://doi.org/10.2166/wcc.2024.319

Birhanu, S. Y., Moges, M. A., Sinshaw, B. G., Tefera, A. K., Atinkut, H. B., Fenta, H. M. & Berihun, M. L. (2022). Hydrological modeling, impact of land-use and land-cover change on hydrological process and sediment yield; case study in Jedeb and Chemoga watersheds. *Energy Nexus*, 5, 100051. https://doi.org/https://doi.org/10.1016/j.nexus.2022.100051

Chanie, K. M. (2024). Hydro-meteorological response to climate change impact in Ethiopia: a review. *Journal of Water and Climate Change*, 15 (4), 1922–1932. https://doi.org/10.2166/wcc.2024.711

Choi, Y. W., Campbell, D. J. & Eltahir, E. A. B. (2023). Near-term regional climate change in East Africa. *Climate Dynamics*, 61, 961–978. https://doi.org/10.1007/s00382-022-06591-9

Chuko, F. W. & Abdissa, A. G. (2023). Impact of land-use dynamics and climate change scenarios on Groundwater recharge in the case of Anger watershed, Ethiopia. *Heliyon*, 9(8). https://doi.org/10.1016/j.heliyon.2023.e18467

Congalton, R. G. & Green, K. (2019). *Assessing the Accuracy of Remotely Sensed Data: Principles and Practices (3rd ed.).* CRC Press, Taylor & Francis Group, LLC.

Daniel, H. (2023). Hydrological response to climate change in the Deme watershed, Omo-Gibe Basin, Ethiopia. *Journal of Water and Climate Change*, 14(4), 1112–1131. https://doi.org/10.2166/wcc.2023.248

Engdaw, K. (2016). *Assessment on Surface Water Potential and Demands of Wabi-shebele Basin in Ethiopia*. MSc. Thesis, Addis Ababa University.

Eva, E. A., Marzen, L. J., Lamba, J., Ahsanullah, S. M. & Mitra, C. (2024). Projection of land use and land cover changes based on land change modeler and integrating both land use land cover and climate change on the hydrological response of Big Creek Lake Watershed, South Alabama. *Journal of Environmental Management*, 370. https://doi.org/10.1016/j.jenvman.2024.122923

FAO. (2023). The State of Food Security and Nutrition in the World 2023. *The State of Food Security and Nutrition in the World 2023*. FAO; IFAD; UNICEF; WFP; WHO; https://doi.org/10.4060/cc3017en.

Feleke, H. G., Amdie, T. A., Rasche, F., Mersha, S. Y. & Brandt, C. (2025). Climate on the Edge: Impacts and Adaptation in Ethiopia's Agriculture. *Sustainability*, 17(11). https://doi.org/10.3390/su17115119

Fita, T. & Abate, B. (2022). Impact of climate change on streamflow of Melka Wakena catchment, Upper Wabi Shebelle sub-basin, south-eastern Ethiopia. *Journal of Water and Climate Change*, 13(5), 1995–2010. https://doi.org/10.2166/wcc.2022.191

Gebisa, B. T. & Dibaba, W. T. (2024). Ensemble modeling of the hydrological impacts of climate change: A case study of the Baro River sub-basin, Ethiopia. *Hydrology Research*, 55(11), 1143–1160. https://doi.org/10.2166/nh.2024.066

Gebrechorkos, S. H., Hülsmann, S. & Bernhofer, C. (2019). Regional climate projections for impact assessment studies in East Africa. *Environmental Research Letters*, 14(4). https://doi.org/10.1088/1748-9326/ab055a.

Gebresellase, S. H., Wu, Z., Xu, H. & Muhammad, W. I. (2023). Scenario-Based LULC Dynamics Projection Using the CA–Markov Model on Upper Awash Basin (UAB), Ethiopia. *Sustainability*, 15(2). https://doi.org/10.3390/su15021683

Gupta, H. V, Kling, H., Yilmaz, K. K. & Martinez, G. F. (2009). Decomposition of the mean squared error and NSE performance criteria : Implications for improving hydrological modelling. *Journal of Hydrology*, 377(1–2), 80–91. https://doi.org/10.1016/j.jhydrol.2009.08.003

Harka, A. E., Roba, N. T. & Kassa, A. K. (2020). Modelling rainfall runoff for identification of suitable water harvesting sites in Dawe River watershed, Wabe Shebelle River basin, Ethiopia. *Journal of Water and Land Development*, 47(1), 186–195. https://doi.org/10.24425/jwld.2020.135313

IPCC (2023). Climate Change 2023: Synthesis Report. Contribution of Working Groups I, II and III to the Sixth Assessment Report of the Intergovernmental Panel on Climate Change. In: P. Arias, M. Bustamante, I. Elgizouli, G. Flato, M. Howden, C. Méndez-Vallejo, J. J. Pereira, R. Pichs-Madruga, S. K. Rose, Y. Saheb, R. Sánchez Rodríguez, D. Ürge-Vorsatz, C. Xiao, N. Yassaa, J. Romero, J. Kim, E. F. Haites, Y. Jung, R. Stavins, … C. Péan (Eds.), *Climate Change 2023 Synthesis Report* (p. 35-51). https://doi.org/10.59327/IPCC/AR6-9789291691647

Kuma, H. G., Feyessa, F. F. & Demissie, T. A. (2022). Land-use/land-cover changes and implications in Southern Ethiopia: evidence from remote sensing and informants. *Heliyon*, 8(3). https://doi.org/10.1016/j.heliyon.2022.e09071.

Lukas, P., Melesse, A. M. & Kenea, T. T. (2025). Integrating Land Use/Land Cover and Climate Change Projections to Assess Future Hydrological Responses: A CMIP6-Based Multi-Scenario Approach in the Omo–Gibe River Basin, Ethiopia. *Climate*, 13(3). https://doi.org/10.3390/cli13030051

Mechal, A. & Bayisa, A. (2025). Modeling the Impacts of Climate Change on Watershed Hydrology Using Climate and Hydrological Models: The Case of the Ziway Lake Watershed, Ethiopian Rift. *Environmental Modeling and Assessment*, 30(3), 515–541. https://doi.org/10.1007/s10666-024-10010-0

Moriasi, D. N., Arnold, J. G., Liew, M. W. Van, Bingner, R. L., Harmel, R. D. & Veith, T. L. (2007). Model Evaluation Guidelines for Systematic Quantification of Accuracy in Watershed Simulations. *ASABE*, 50(3), 885–900.

Nash, J. E. & Sutcliffe, I. V. (1970). River Flow Forecasting Through Conceptual Models Part I - A Discussion of Principles. *Journal of Hydrology*, 10, 82–290.

Omay, P. O., Muthama, N. J., Oludhe, C., Kinama, J. M., Artan, G. & Atheru, Z. (2023). Evaluation of CMIP6 historical simulations over IGAD region of Eastern Africa. *Discover Environment*, 1(1). https://doi.org/10.1007/s44274-023-00012-2

Rathjens, H., Bieger, K., Srinivasan, R., Chaubey, I. & Arnold, J. G. (2016). *CMhyd User Manual: Documentation for preparing simulated climate change data for hydrologic impact studies*. http://swat.tamu.edu/software/cmhyd/.

Riahi, K., van Vuuren, D. P., Kriegler, E., Edmonds, J., O'Neill, B. C., Fujimori, S., Bauer, N., Calvin, K., Dellink, R., Fricko, O., Lutz, W., Popp, A., Cuaresma, J. C., KC, S., Leimbach, M., Jiang, L., Kram, T., Rao, S., Emmerling, J., …Tavoni, M. (2017). The Shared Socioeconomic Pathways and their energy, land use, and greenhouse gas emissions implications: An overview. *Global Environmental Change*, 42, 153–168. https://doi.org/10.1016/j.gloenvcha.2016.05.009

Roba, N. T., Kassa, A. K., Geleta, D. Y. & Harka, A. E. (2021). Streamflow and sediment yield estimation, and area prioritization for better conservation planning in the Dawe River watershed of the Wabi Shebelle River Basin, Ethiopia. *Heliyon*, 7(12). https://doi.org/10.1016/j.heliyon.2021.e08509

Rwanga, S. S. & Ndambuki, J. M. (2017). Accuracy Assessment of Land Use/Land Cover Classification Using Remote Sensing and GIS. *International Journal of Geosciences*, 8, 611–622. https://doi.org/https://doi.org/10.4236/ijg.2017.84033

Seifu, T. K. & Eshetu, K. D. (2024). Characterizing the aridity indices and potential evapotranspiration using CMIP6-GCMs in two distinct regions of Ethiopia. *Journal of Water and Climate Change*, 15(4), 1507–1531. https://doi.org/10.2166/wcc.2024.394

Semegnew, T., Soromessa, T. & Bekele, T. (2021). Analysis of the Current and Future Prediction of Land Use/Land Cover Change Using Remote Sensing and the CA-Markov Model in Majang Forest Biosphere Reserves of Gambella, Southwestern Ethiopia. *Scientific World Journal*, 2021.

https://doi.org/https://doi.org/10.1155/2021/6685045

Shah, M. M., Fischer, G., & van Velthuizen, H. (2008). Food security and sustainable agriculture: The challenges of climate change in Sub-Saharan Africa.

Siraj, B., Moges, A. & Dananto, M. (2023). Trend analysis, past dynamics and future prediction of land use and land cover change in upper Wabe-Shebele river basin. *Heliyon*, 9(9). https://doi.org/10.1016/j.heliyon.2023.e19128

Tofu, D. A., Mekuria, M. M. & Ogato, G. S. (2023). Climatic extremes' resilient livelihoods of rural households in the Eastern Ethiopia. *Agriculture and Food Security*, 12(1). https://doi.org/https://doi.org/10.1186/s40066-023-00446-0.

Truneh, L. A., Matula, S. & Báťková, K. (2024). An analysis of the impacts of land use change on the components of the water balance in the Central Rift Valley sub-basins in Ethiopia. *Sustainable Water Resources Management*, 10(2). https://doi.org/10.1007/s40899-024-01050-1

Woldemariam, G. W., Iguala, A. D., Tekalign, S. & Reddy, R. U. (2018). Spatial Modeling of Soil Erosion Risk and Its Implication for Conservation Planning: The Case of the Gobele Watershed, East Hararghe Zone, Ethiopia. *Land*, 7(25). https://doi.org/10.3390/land7010025

Woldu, T. T., Ayenew, T., Baychken, B. & Birhanu, B. (2024). Spatiotemporal recharge estimation in the upper Awash sub-basin, central Ethiopia. *Hydrology Research*, 55(7), 711–727. https://doi.org/10.2166/nh.2024.164

Wudineh, F. A. (2023). Land-use and land-cover change and its impact on flood hazard occurrence in Wabi Shebele River Basin of Ethiopia. *Hydrology Research*, 54(6), 756–769. https://doi.org/https://doi.org/10.2166/nh.2023.121

Xiang, X., Ao, T., Xiao, Q., Li, X., Zhou, L., Chen, Y., Bi, Y. & Guo, J. (2022). Parameter Sensitivity Analysis of SWAT Modeling in the Upper Heihe River Basin Using Four Typical Approaches. *Applied Sciences*, 12(19). https://doi.org/10.3390/app12199862

Yaekob, T., Tamene, L., Gebrehiwot, S. G., Demissie, S. S., Adimassu, Z., Woldearegay, K., Mekonnen, K., Amede, T., Abera, W., Recha, J. W., Solomon, D. & Thorne, P. (2022). Assessing the impacts of different land uses and soil and water conservation interventions on runoff and sediment yield at different scales in the central highlands of Ethiopia. *Renewable Agriculture and Food Systems*, 37, S73–S87. https://doi.org/10.1017/S1742170520000010

Yang, L., Shi, L., Li, J. & Kong, H. (2024). Spatio-temporal pattern change of LULC and its response to climate in the Loess Plateau, China. *Scientific Reports*, 14(1). https://doi.org/10.1038/s41598-024-73945-0

Yilmaz, B., Aras, E. & Nacar, S. (2024). A CMIP6-ensemble-based evaluation of precipitation and temperature projections. *Theoretical and Applied Climatology*, 155(8), 7377–7401. https://doi.org/10.1007/s00704-024-05066-7.

Zeleke, T., Beyene, F., Deressa, T., Yousuf, J. & Kebede, T. (2021). Vulnerability of smallholder farmers to climate change-induced shocks in east hararghe zone, ethiopia. *Sustainability*, 13(4), 1–19. https://doi.org/10.3390/su1304216.